Fuel 235 (2019) 595–602

Contents lists available at ScienceDirect

Fuel

journal homepage: www.elsevier.com/locate/fuel

Full Length Article

Vision based algorithm for automated determination of smoke point of diesel blends

Guilllermo Rubio-Gomez, Lis Corral-Gomez, Jose Antonio Soriano, Arantzazu Gomez, Fernando J. Castillo-Garcia*

School of Industrial Engineering, University of Castilla-La Mancha, Av. Carlos III, Real Fabrica de Armas, 45071 Toledo, Spain

ARTICLE INFO

Keywords:
Smoke point
Threshold sooting index
Sooting tendency
Automated method
Image processing

ABSTRACT

Current regulations restrict NOx and particulate emissions (PM) produced by new vehicles. One solution for reducing these emissions, mainly PM, is focused on the use of cleaner fuels. In this sense, the smoke point test (SP) has been proved to be a fast tool when comparing the sooting tendency of fuels. As manual SP determination can imply an error owing to the inherent uncertainty of visual flame observation, the updated ASTM D1322-18 has stated that the new commercial equipment SP10 Automated Smoke Point Analyser is the reference for SP determination. However, its high cost has motivated this work where a vision based algorithm for automated determination of SP without wick-fed modifications is proposed. Experimental results demonstrate the accuracy and repeatability of the proposed method.

1. Introduction

Along the history, compression ignition engines have shown higher energy conversion efficiency than spark ignition engines but a higher production of nitrogen oxides (NOx) and particulate matter (PM), not only in mass terms but also in number, are observed in both, steady state and transient conditions [1]. However, although PM was not concerning in spark ignition engines, nowadays the new direct injection engines show a quite high particulate emission [2]. In this way, the current regulations Euro 6 and the US 2010 restrict NOx and PM emissions produced by new vehicles, in Europe and USA, respectively [3,4].

One solution for reducing vehicles pollutant emissions, mainly PM, is focused on the use of cleaner fuels. Although the opacity and, therefore, engine particle emissions, depend on the fuel and engine conditions, the smoke point (SP) test has been proved to be a fast tool when comparing the sooting tendency of different fuels [5–8].

Smoke point is defined as the height in millimetres of the highest flame produced without smoking when the fuel is burned in a specific wick-fed test lamp. Therefore, as higher is the flame height, lower is the tendency to smoke of the tested fuel [9].

Manual SP determination can imply errors due to the inherent uncertainty of visual flame observation. In order to narrow down the error, the Test Method D1322 for measuring manually the smoke point fixes a repeatability between results obtained by the same operator of 2 mm, whereas the reproducibility (difference between results obtained by different operators) must be lower than 3 mm [9].

However, uncertainties can be minimized if direct visual observation is avoided by means of an automatic determination of the SP. Watson et al. [10] developed a test based on the fuel uptake rate (determined using an analytical balance) and image analysis of videos recorded with a webcam, rather than the height of the flame. In this work a conventional Logitech 9000 webcam is used for estimating flame height at 20 frames per second. The acquired images are processed using Matlab. A binarization of the color image is used before determining tip position and the flame height on the black and white image. A rod is inserted into the wick sheath for image calibration purposes. Results showed that reproducibility was improved. However, the smoke point lamp was to be redesigned.

Graziano et al. [11] also used the fuel uptake rate but the commercial webcam was replaced by a CCD camera for registering soot luminosity using a recording interval of 1 s. This work establishes that using a fixed intensity threshold significantly affects the flame detection and an intensity gradient approach is therefore used to perform the image processing.

An automated determination of the SP was also developed by Pino et al. [12] but a Gulder burner was used instead of an ASTM wick-fed lamp. Recently, ASTM D1322-18 has stated that the new commercial equipment, *SP10 Automated Smoke Point Analyser* is the reference for SP determination. This equipment uses a vision system and a balance for

* Corresponding author.
E-mail address: Fernando.Castillo@uclm.es (F.J. Castillo-Garcia).

https://doi.org/10.1016/j.fuel.2018.08.032
Received 25 February 2018; Received in revised form 3 August 2018; Accepted 7 August 2018
Available online 17 August 2018

determining SP value.

Some other methodologies for estimating the sooting tendency of fuels can be also found in literature for avoiding visual observation uncertainties, but they are not based on smoke point measurements [13–15].

In this work, a new approach for automation of an ASTM smoke point lamp has been developed. The proposed method is based on image processing not only for measuring the flame height, as FURTI based methods [10,11], but also for determining the flame tip deformation during the experiments, without requiring any additional equipment as analytical balance for SP determination. The novel commercial equipment, *SP10 Automated Smoke Point Analyser*, provides accurate SP values but is a high cost equipment since the proposed method here only implies slight and cheap lamp modifications.

This paper is structured as follows: Section 2 details the experimental platform and the vision based algorithm for obtaining SP since Section 3 shows the experimental results and the discussions.

2. Materials and methods

The main part for SP determination is ASTM D1322 standardized test diffusive lamp (see Fig. 1).

A conventional experiment is performed by the following procedure:

- Fuel tank is filled with diesel fuel to be characterized.
- Wick is lighted.
- Fuel tank nut is manually rotated to increase flame height.
- Operator watch the flame attempting to note when it starts producing smoke.

Following this procedure, Smoke Point is the last value of flame height before smoke is produced [9].

Obviously, ASTM D1322 norm take into account the inherent observer errors and establishes a sensibility of 0.5 mm, i.e. the observed SP must be rounded to the nearest 0.5 mm scale line (see Fig. 1b). In addition, the experiment must be carried out 3 times and, if these values vary over a range greater than 1.0 mm, the test must be rejected.

It is important to mention that ASTM D1322 norm describes all the overall requirements before experiments (ambient specification, lamp orientation, etc.) and the procedure to calibrate it (see [9] for more details).

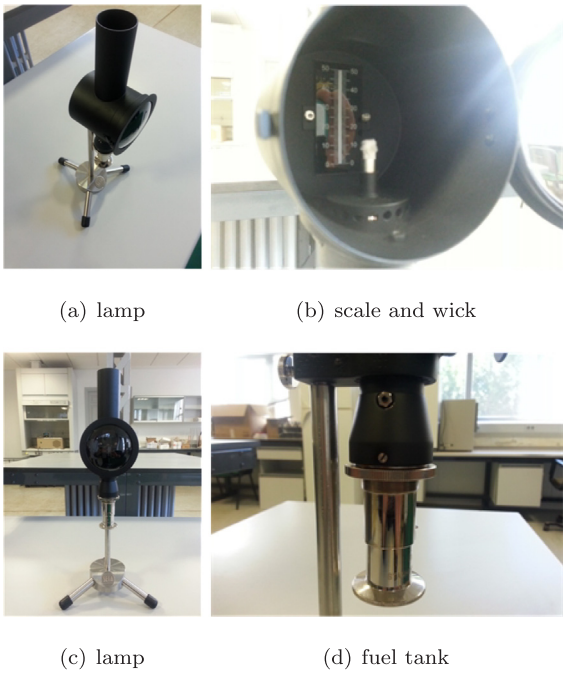

(a) lamp (b) scale and wick

(c) lamp (d) fuel tank

Fig. 1. ASTM D1322 standarized lamp.

The aforementioned normalized test lamp has been adapted in order to automate the smoke point test procedure, that used to be carried out manually as specified in [9]. No modification to the lamp is made during the adaptation process, this is due to its normalized specifications and calibration. A novel image processing based algorithm has been developed to automatically determine smoke point after recording the flame evolution process.

The main goal of this automation is to carry out the test at a steady and controlled speed while automatically recording the flame evolution. Irregularities in test speed, due to its manual, cause sudden variations in flame height that difficult the SP automatic detection process. This adaptation also allows to isolate the lamp from air perturbations that could come from the surroundings, by placing the platform inside a container. The user can control the test externally via PC by means of a *Matlab* application.

2.1. Materials

In order to implement this platform, a mechanical actuator is attached to the lamp nut. The required speed for lamp actuator has been determined to lay between 1 and 3 rpm and the needed torque to rotate lamp actuator is about 3 Nm. Taking into account the requirements of the lamp, low speed and relatively high torque, the selected mechanical actuator is a continuous rotation servomotor [16] model *SM-S4303R* from *SPRINGRC*. This servomotor is shown in Fig. 2, and provides the characteristics required by the lamp.

To attach the servomotor to the lamp actuator, a reduction gearbox has been designed, both to adapt the speed of the servomotor (5–50 rpm) to the lamp speed and to amplify the torque given by the servomotor (0.4 Nm). The gearbox was designed to give a speed reduction of 15.6: 1. A sketch of the design can be seen in Fig. 3. The gearbox has been built by 3D impression in Polylactic Acid (PLA). Pictures of the printed gearbox can be seen in Fig. 4. This mechanical device is controlled by means of an *Arduino*™ board model *Mega 2560*.

The hardware used to record the flame evolution during the test is a web camera model *C270* from *Logitech*®, see Fig. 5. It offers a resolution of 1280 × 960. The image format employed is *RGB24*.

Finally, all the materials are attached to the normalized test lamp. The camera is placed in the top of the gearbox, attached by a structure that keeps it firmly aligned with the lamp at a distance of 20 mm. This fastening device was printed in PLA and is shown in Fig. 6.

Another gear, attached to the lamp nut, has been built to transmit the movement from the gearbox. A sheet of steel is used to give strength and stability to all components of the automated smoke point test platform. The final assembly can be seen in Fig. 7.

2.2. Smoke point detection algorithm

A new image processing based method for automated smoke point detection is proposed. Other works which applied computer vision for

Fig. 2. *SM-S4303R* servomotor from *SPRINGRC*.

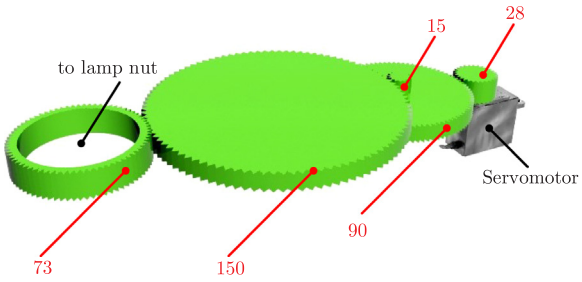

Fig. 3. Sketch of the designed gearbox.

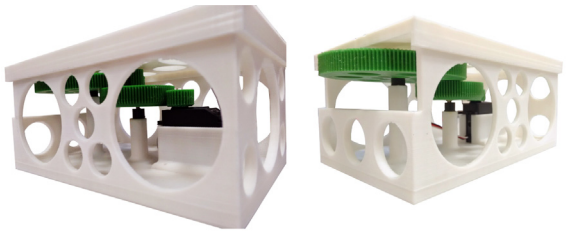

(a) Detail View (b) Detail View

(c) Sideways View (d) Superior View

Fig. 4. Gearbox developed.

Fig. 5. Web camera *C270* from *Logitech®*.

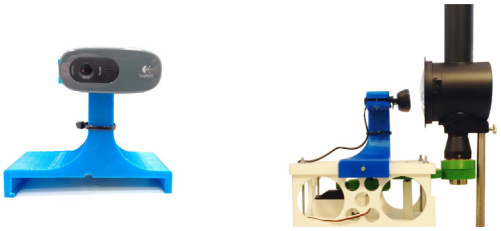

(a) Frontal View (b) Sideways View

Fig. 6. Camera fastening structure.

detecting or characterizing flame can be found (e.g. [17,18] but this is the first work which applied computer vision for automated detection of Smoke Point. Complete explanation of the image acquisition and analysis process is given, followed by the description of the algorithm proposed for the detection.

(a) General view (b) Sideways view

Fig. 7. Overview of the automatized test platform.

2.2.1. *Image acquisition*

Camera resolution is set to the maximum allowed one, 1280 × 960. Placing the camera 20 mm away from the flame, a resolution of 0.05 mm per pixel is obtained. Taking into account that the tolerance in the determination of the SP allowed by the norm [9] is 0.5 mm, the resolution obtained is considered adequate for this purpose. Frame rate is set to 20 frames per second. Images are acquired in RGB format (each pixel contains three values for red, green and blue that take a value between 0 and 255) [19]. The luminous characteristics of flames make it easier to identify its shape. However, in order to deal with the high luminous intensity of the flame, exposure time is reduced to minimum and therefore a near to binary image is obtained. Fig. 8 shows a flame image acquired. The entire flame evolution during the smoke point test, from low flame height until smoke point has been passed, is recorded. The video acquired is then analyzed to automatically detect the flame height at SP.

2.2.2. *Image analysis*

First step in image analysis is convert the image to grayscale format. It means that each pixel take a value of luminous intensity from 0 to 255, being 0 pure black and 255 pure white. This process is carried out by computing a weighted sum with the colour channels of the image in RGB format [20]. Weights of red, green and blue respectively are 0.299, 0.587 and 0.114 [21]. The resulting image can be seen in Fig. 9.

A threshold binarization technique is then applied to the grayscale image to obtain a binary image where each pixel have a value of high or low [22]. It consists in assign a high value to the pixels with a luminous intensity above a certain level, and low value to the ones with a luminous intensity below that level. Pixels with high binary level correspond to the image areas where the flame is present. Since flame luminosity is quite steady, there is no need to compute threshold level for each image acquired. Luminosity in the different regions of the flame

Fig. 8. Flame image acquired.

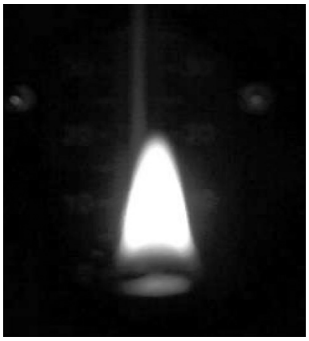

Fig. 9. Flame image converted to grayscale.

has been analyzed for flames at different heights, see Fig. 10.

Threshold luminous intensity level of 90 (35% of 255) is observed to determine well the flame shape, see Fig. 11.

After binarization, basic filter operations like area filter or holes filling are carried out [23]. Area filter are computed by giving low level to such groups of pixels with an area below a certain limit, defined by the area of the smallest flame. Holes filling consist on give a high level to any group with low level surrounded by high level pixels. The result of this filters is shown in Fig. 12.

Once the image has been converted to a binary matrix, the shape of the flame is obtained as the contour of the areas with high binary levels.

2.2.3. Flame characterisation

The evolution of the flame shape during the smoke point test has been analyzed in order to detect significant changes in its geometry, specially on the tip, which indicates the smoke point, as specified in [9]. Two flame shape characteristic parameters have been defined.

- Tip Ratio, R_t. Firstly, we need to introduce Flame tip. Flame tip is determined by obtaining the flame core, with a higher luminous intensity level threshold of 230 (90% of 255). Obtaining flame core from the high luminous intensity area of the flame ensures the location of the geometrical centre of the flame. Flame tip is obtained from the top flame edge, centred in the middle point of the core and with a length of 40% the width of the bottom flame edge, that figure is determined after several experimental tests. The width and the height of the flame tip are W_t and H_t, respectively, and therefore the Tip Ratio, R_t of the flame tip can be defined by:

$$R_t = \frac{H_t}{W_t} \tag{1}$$

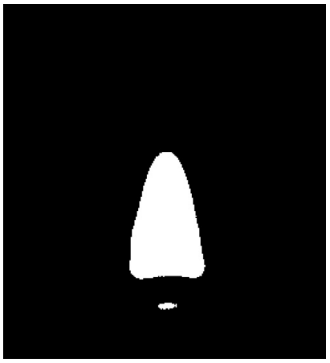

Fig. 11. Flame binary image with 35% luminosity level threshold.

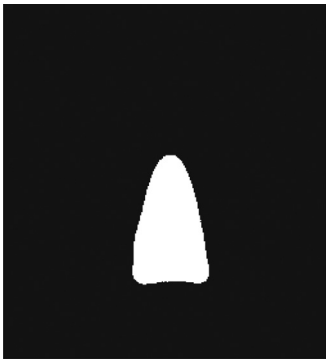

Fig. 12. Flame binary image after filters.

- Flame height, H_f, which corresponds to the total height of the Flame shape.

Fig. 13 represents these parameters for flame geometric characterisation.

After multiple experiments, we realize that the evolution of Tip Ratio, R_t against Flame Height, H_f has two parts with clear linearity, separated by a point where the slope increases. After experimentation, that point of linearity break is observed to correspond to the SP height. This change in the slope is employed to detect the smoke by analyzing the data obtained from the test. Different speeds for the lamp nut are experimentally tested in order to maximize the change in slope and thus make the smoke point easier to detect. Speeds of 1, 2 and 3 rpm for the lamp actuator are tested.

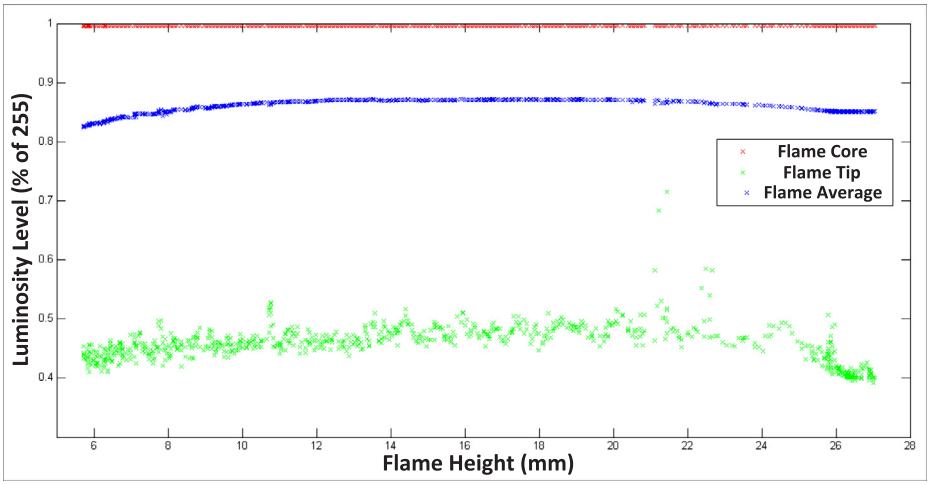

Fig. 10. Luminous Intensity of flame regions during a complete test.

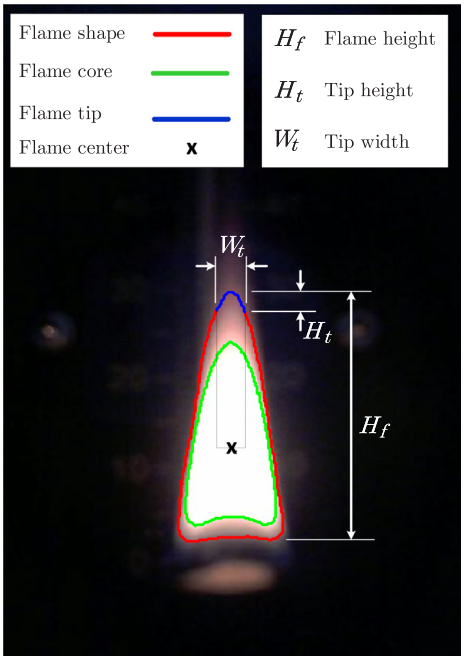

Fig. 13. Regions defined for flame characterisation.

In Fig. 14 slope change in the relation between Tip Ratio and total flame height for different test speeds is shown. As can be observed, speed of 3 rpm maximizes the change and therefore is chosen as test speed for smoke point automatic detection.

2.2.4. Detection algorithm proposed

Several processes are perform with data from the plot of the Tip Ratio against total flame height to determine the flame height corresponding to the smoke point.

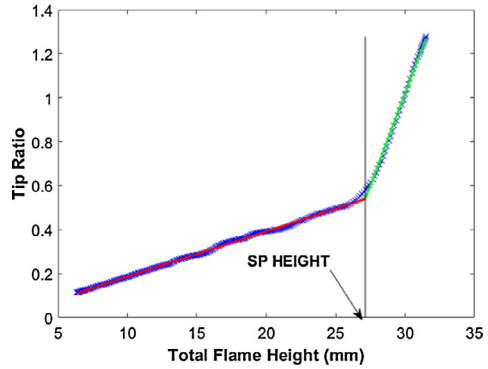

Fig. 15. Data Filtering Process.

First step consists on some basic filters of the data. Initially, points above (or below) the addition (or subtraction) of the mean and the standard deviation of the data are first disregarded. Then, a mobile-weighted-mean filter is applied. This filter consist on giving to each point the value of a weighted sum computed from the neighbours values. The number of values used for the sum have been experimentally set to 9. Weights for the sum are determined by minimizing the error obtained in the detection, resulting the following discrete filter equation:

$$H_f(k) = \sum_{n=-4}^{4} a_n \cdot H_f(k-n) \tag{2}$$

where $a_{-4} = a_4 = 0.04$, $a_{-3} = a_3 = 0.08$, $a_{-2} = a_2 = 0.12$, $a_{-1} = a_1 = 0.16$ and $a_0 = 0.2$ (Note that the sum of a_i is 1).

Finally, points at highest heights, that show a distortion caused by the apparition of smoke in the flame, are also disregarded. The results of these filters are shown in Fig. 15.

Once the data have been filtered, two first order curves are fitted to the points which shown linearity, corresponding to such before and

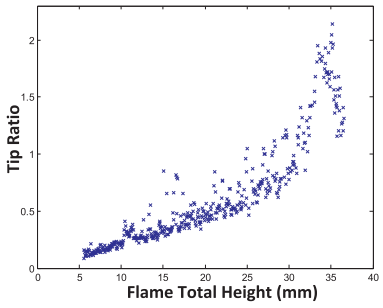

(a) Original Data

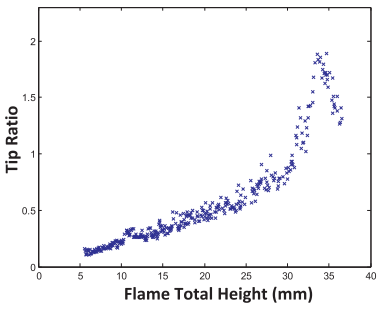

(b) Data after disregarding noise

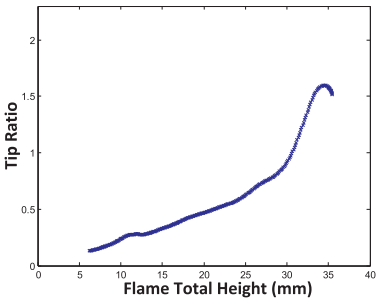

(c) Data after mobile-weighted-mean filter

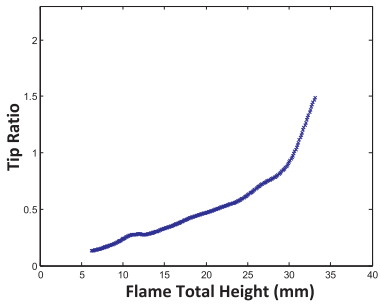

(d) Elimination of deformation caused by smoke production

Fig. 14. Tip Ratio vs Flame height for different test speeds.

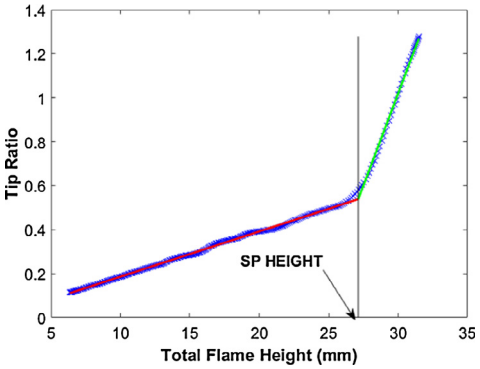

Fig. 16. First order curves fitted and calculated SP height.

after the SP height. The x coordinate where these two curves meet correspond to the SP height. These first order curves and the computed SP height can be seen in Fig. 16.

3. Results and discussion

3.1. Experimental procedure

In this Section, two different results will be shown. First ones are related to the SP determination process. Some reference fuels are tested and their SP values are compared to the standard one at 101.3 kPa. However, as Smoke Point values depend of the particular lamp, a new set of tests based on the Threshold Sooting Index (TSI) determination were made and compared with literature. These TSI results were directly determined by using the automated SP values and are compared to [11] for validation purposes.

In order to eliminate possible interference in the tests, several considerations were taken into account:

- Experimental platform is placed in a wind isolated vessel, thus avoiding air currents interfering with the flame.
- Tests were performed during a week with steady weather conditions, so that no sharp pressure changes occur between tests.
- Test were carried out at a laboratory with an operating ambient temperature of 25 ° C± 1 °C.

3.2. SP results

In order to verify both the precision and the repeatability of the proposed algorithm, tests with standardized fuels were carried out. These fuels, binary blends of toluene and 2,2,4-trimethylpentane (iso-octane) are summarized in Table 1 together with their standard SP values at 101.3 kPa.

Three consecutive SP measures of each fuel blend were made. The average value of SP together with the total and relative error regarding to the standard value are also included in Table 1. Fig. 17 represents the obtained results and the absolute error.

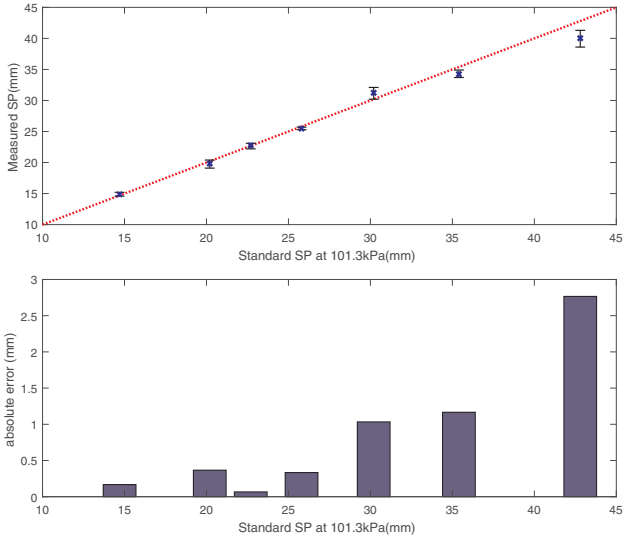

Fig. 17. SP experiments: results summary.

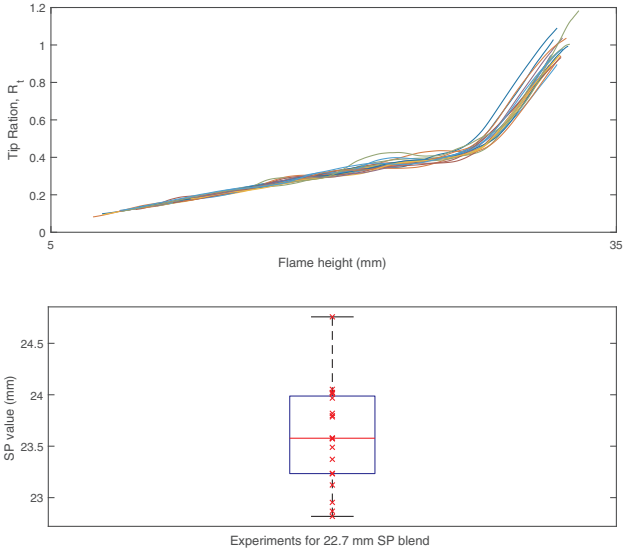

Fig. 18. Repeteability test for 20% (v/v) teluene – 80% (v/v) iso-octane blend. (a) Tip Ratio vs. Flame Height. (b) Box Plot results.

As can be seen, the proposed method yields a high precision for fuel blends with SP in the low and medium range, with less than 0.5 mm of absolute error.

Finally, some repeatability tests have been carried out to check the proposed method. A 20% (v/v) toluene 80% (v/v) iso-octane blend with 22.7 mm of standard SP value has been chosen for this experiment. Repeatability tests are performed by taking 10 consecutive measurements of this fuel blend. Test results are shown in Fig. 18. Fig. 18a

Table 1
SP experiments: results summary

Blend	Standard SP at 101.3 kPa (mm)	Test 1 (mm)	Test 2 (mm)	Test 3 (mm)	Mean (mm)	Absolute error (mm)	Relative Error (%)
40% (v/v) toluene 60% (v/v) iso-octane	14.7	15.2	14.8	14.6	14.9	0.17	1.13
25% (v/v) toluene 75% (v/v) iso-octane	20.2	20.0	19.1	20.4	19.9	0.37	1.82
20% (v/v) toluene 80% (v/v) iso-octane	22.7	23.0	23.1	22.2	22.8	0.07	0.29
15% (v/v) toluene 85% (v/v) iso-octane	25.8	25.3	25.7	25.4	25.5	0.33	1.29
10% (v/v) toluene 90% (v/v) iso-octane	30.2	31.4	30.2	32.1	31.2	1.03	3.42
5% (v/v) toluene 95% (v/v) iso-octane	35.4	33.7	34.1	34.9	34.2	1.17	3.30
0% (v/v) toluene 100% (v/v) iso-octane	42.8	38.6	41.3	40.2	40.0	2.77	6.46

Table 2
Blends for TSI determination.

Blend	TSI (Graziano et al. [11])	TSI (proposed method)	Absolute error (mm)	Relative error (%)
35% (v/v) toluene 65% (v/v) n-heptane (BB)	15.18	15.58	0.40	2.66
10% (v/v) bencene 90% (v/v) BB	17.19	16.78	0.41	2.38
20% (v/v) bencene 80% (v/v) BB	20.11	18.16	1.95	9.71
40% (v/v) bencene 60% (v/v) BB	23.18	22.84	0.34	1.48
15% (v/v) 1-methylnaphtalene 85% (v/v) BB	26.87	26.47	0.40	1.48
10% (v/v) 1-methylnaphtalene 90% (v/v) BB	22.58	24.69	2.11	9.36
5% (v/v) 1-methylnaphtalene 95% (v/v) BB	19.07	19.00	0.07	0.38
10% (v/v) toluene 90% (v/v) n-heptane	7.51	8.12	0.61	8.11
20% (v/v) toluene 80% (v/v) n-heptane	9.71	9.87	0.16	1.63
40% (v/v) toluene 60% (v/v) n-heptane	16.87	17.67	0.80	4.76
100% (v/v) iso-octane	8.30	9.24	0.90	10.76
5% (v/v) toluene 95% (v/v) iso-octane	10.00	10.15	0.15	1.51
10% (v/v) toluene 90% (v/v) iso-octane	13.70	12.85	0.85	6.20
20% (v/v) toluene 80% (v/v) iso-octane	15.80	15.32	0.48	3.04
40% (v/v) toluene 60% (v/v) iso-octane	21.30	22.56	1.26	5.93

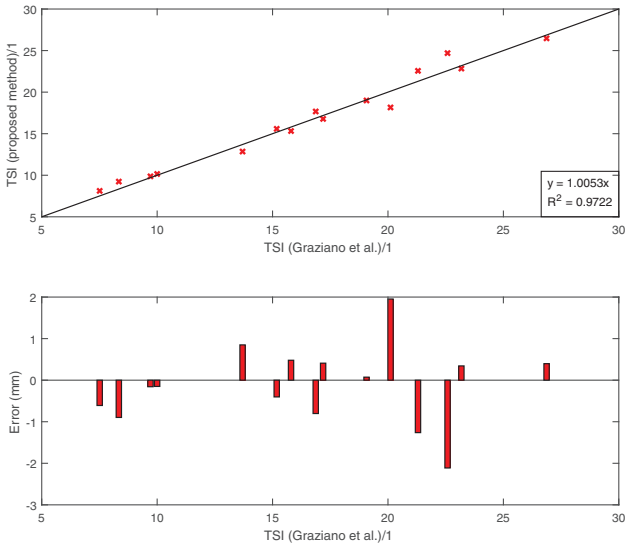

Fig. 19. TSI results: Graziano et al. [11] vs. proposed method.

compare all the Flame Height evolution against Tip Ratio, since Fig. 18b represents the Box Plot results. [24].

3.3. TSI results

Fuel molecular weight affects the sooting tendency when the smoke point lamp is used, since its increase makes necessary more oxygen to diffuse into the flame [25]. The experimental Threshold Sooting Index described as Eq. (3) is therefore used:

$$TSI = a\left(\frac{MW}{SP}\right) + b \tag{3}$$

where MW is the molecular weight of fuel ($g \cdot mol^{-1}$), and a and b are apparatus-dependent constants.

As specified in the ASTM D1322, the following two blends with standardized smoke points were chosen for lamp calibration (f factor): 40% (v/v) toluene 60% (v/v) iso-octane and 20% (v/v) toluene 80% (v/v) iso-octane. As in different works [6,11,26], the TSI scale stated by Olson et al. [27] was used for determining the lamp constants a and b. A final values of 3.4847 mol/g·mm and −1.5 were obtained, respectively.

In order to validate the algorithm, different binary and ternary blends were tested and compared with results obtained in literature [11]. Three sets with three tests on each were made in consecutive days. Table 2 shows the different blends to be tested including the TSI average results. The regression in Fig. 19, with a correlation coefficient of 97.22%, confirms the goodness of the results obtained.

4. Conclusions

In this paper a new vision based algorithm for automated determination of SP value has been developed.

Using a low cost platform, a normalized ASTM D1322 lamp has been adapted to be automatically actuated by means of a servomotor and a self-made gearbox.

Using a conventional webcam the flame image is captured and filtered in order to characterize the flame during the experiments.

The Smoke Point can be automatically obtained by analyzing the evolution of Tip Ratio against Flame Height.

A first set of experiments checked the accuracy and repeatability of the proposed method when determining the SP.

A second set of experiments, where TSI results of 15 different binary and ternary blends were compared with literature, were made for validating the proposed vision based algorithm. The high correlation confirms the goodness of the methodology.

The main advantage of this method is the reduction of inherent error caused by operators criteria during the tests and the reduction of the test time. Although ASTM D1322 now states that *SP10* is the reference for SP determination, its high cost can be considered a barrier for its extended use. The solution proposed here open a door for developing a low-cost equipment for automated SP determination.

Acknowledgement

Authors wish to thank the financial support of the Spanish Ministry of Economy and Competitiveness to project POWER (ENE2014-57043-R).

References

[1] Heywood JB, et al. Internal combustion engine fundamentals.
[2] Überall A, Otte R, Eilts P, Krahl J. A literature research about particle emissions from engines with direct gasoline injection and the potential to reduce these emissions. Fuel 2015;147:203–7.
[3] Emission standards. EU: Cars and Light Trucks.https://www.dieselnet.com.
[4] Emission standards. United States: Cars and Light-Duty Trucks: Tier 3.https://www.dieselnet.com.
[5] Armas O, Gomez MA, Barrientos EJ, Boehman AL. Estimation of opacity tendency of ethanol – and biodiesel-diesel blends by means of the smoke point technique. Energy Fuels 2011;25(7):3283–8.
[6] Barrientos EJ, Lapuerta M, Boehman AL. Group additivity in soot formation for the example of c-5 oxygenated hydrocarbon fuels. Combust Flame 2013;160(8):1484–98.
[7] Barrientos EJ, Anderson JE, Maricq MM, Boehman AL. Particulate matter indices using fuel smoke point for vehicle emissions with gasoline, ethanol blends, and butanol blends. Combust Flame 2016;167:308–19.
[8] Gómez A, Soriano J, Armas O. Evaluation of sooting tendency of different

oxygenated and paraffinic fuels blended with diesel fuel. Fuel 2016;184:536–43.
[9] ASTM Standard D1322. Standard test method for smoke point of kerosine and aviation turbine fuel; 2002.
[10] Watson RJ, Botero ML, Ness CJ, Morgan NM, Kraft M. An improved methodology for determining threshold sooting indices from smoke point lamps. Fuel 2013;111:120–30.
[11] Graziano B, Ottenwalder T, Manderfeld D, Pischinger S, Grunefeld G. Advanced methodology for the detection of smoke point heights in hydrocarbon flames. Energy Fuels 2018;32(3):3908–19.
[12] Pino J, Garcés HO, Cuevas J, Arias LE, Rojas AJ, Fuentes A. Soot propensity by image magnification and artificial intelligence. Fuel 2018;225:256–65.
[13] McEnally CS, Pfefferle LD. Improved sooting tendency measurements for aromatic hydrocarbons and their implications for naphthalene formation pathways. Combust Flame 2007;148(4):210–22.
[14] Lemaire R, Lapalme D, Seers P. Analysis of the sooting propensity of c-4 and c-5 oxygenates: comparison of sooting indexes issued from laser-based experiments and group additivity approaches. Combust Flame 2015;162(9):3140–55.
[15] Crossley SP, Alvarez WE, Resasco DE. Novel micropyrolyis index (mpi) to estimate the sooting tendency of fuels. Energy Fuels 2008;22(4):2455–64.
[16] Bianculli AJ. Stepper motors: application and selection. IEEE Spectrum 7(12).
[17] Töreyin BU, Dedeoğlu Y, Güdükbay U, Cetin AE. Computer vision based method for real-time fire and flame detection. Pattern Recogn Lett 2006;27(1):49–58.
[18] Horng W-B, Peng J-W, Chen C-Y. A new image-based real-time flame detection method using color analysis. Networking, Sensing and Control, 2005. Proceedings. 2005 IEEE. IEEE; 2005. p. 100–5.
[19] Forsyth DA, Ponce J. Computer vision: a modern approach. Prentice Hall Professional Technical Reference; 2002.
[20] Liu W, Zeng W, Dong L, Yao Q. Efficient compression of encrypted grayscale images. IEEE Trans Image Process 2010;19(4):1097–102.
[21] International Communication Union. Recommendation ITU-R BT.601-7; 2011.
[22] Sezgin M, Sankur B. Survey over image thresholding techniques and quantitative performance evaluation. J Electron Imaging 2004;13(1):146–66.
[23] Jensen JR, Lulla K. Introductory digital image processing: a remote sensing perspective.
[24] Williamson DF, Parker RA, Kendrick JS. The box plot: a simple visual method to interpret data. Ann Internal Med 1989;110(11):916–21.
[25] Calcote H, Manos D. Effect of molecular structure on incipient soot formation. Combust Flame 1983;49(1–3):289–304.
[26] Mensch A, Santoro RJ, Litzinger TA, Lee S-Y. Sooting characteristics of surrogates for jet fuels. Combust Flame 2010;157(6):1097–105.
[27] Olson D, Pickens J, Gill R. The effects of molecular structure on soot formation ii. diffusion flames. Combust Flame 1985;62(1):43–60.